Chalcogenide Letters Vol. 21, No. 6, June 2024, p. 449 - 458

Computational study of Cd-based chalcogenide spinels $CdSm_2(S/Se)_4$ for spintronic applications

S. Maqsood[a,*], M. A. Javed[b], S. Mumtaz[c], Mohammad K. Al-Sadoon[d]
[a]*Centre for Advanced Studies in Physics (CASP), GC University, Lahore -54000*
[b]*Department of Mathematics, GC University, Lahore -54000, Pakistan*
[c]*Department of Electrical and Biological Physics, Kwangwoon University, Seoul 01897, South Korea*
[d] *Department of Zoology, College of Science, King Saud University, P.O. Box 2455, Riyadh 11451, Saudi Arabia*

In this letter, first-principle computations are utilized in order to explore the Cd-based chalcogenide spinels $CdSm_2(S/Se)_4$ spinels. Generalized gradient approximation (PBEsol-GGA) and modified Becke-Johnson potential (mBJ) are used to calculate structural, mechanical, spin-polarized electronic and magnetic features. The optimization analysis demonstrates that ferromagnetic contends of both chalcogenides releases a greater amount of energy than the anti-ferromagnetic contends. Further, structural and thermodynamic stability are justified through the calculations Born stability criteria and formation energy. Additionally, mechanical features indicate both chalcogenides are ductile in nature through calculations of Poisson's and Pugh ratios. Curie temperature (Tc) in terms of Heisenberg simulation and the corresponding density of states is also calculated for ferromagnetic stability of both chalcogenides. Spin polarized electrical characteristics that are spin-polarized are indicative of a half-metallic ferromagnetic nature (spin-down indicates the semiconductor nature, while the spin-up is metallic nature). Total magnetic moments of both chalcogenides are appear due to hybridization of f-states of rare earth (Sm) element and p-states of chalcogenides.

(Received March 7, 2024; Accepted June 4, 2024)

Keywords: Cd-based chalcogenides, DFT calculations, Mechanical features, Half-metallic ferromagnetism, Magnetic moments.

1. Introduction

Pertaining to their multifaceted applications in energy storage, microwave adsorption, the photo-catalysis, and nano-structured magnetic compounds, nano-sized ferrites of spinel (NSFs) in particular demonstrate captivating characteristics [1-3]. The chalcogenides AB_2X_4 mathematical model of NSFs potentially denotes the cubic arrangement of chalcogenide ions. The diagram in (A) illustrates the tetrahydral intervening sites, whereas [B] depicts octahedral locations of greater magnitude. Both of the locations are occupied by cations, which occupy the octahedral and tetrahedral spots with a divalent element and trivalent ions, respectively [4]. All of the cations occupying the octagonal structured positions possess identically aligned moments of magnetic attraction. On the contrary, the magnetic moments of the cations located at tetrahedral spots are oppositely oriented to those observed at octahedral placements. Notably, the aggregate magnetism of spinel ferrites is attributable to two of these dipoles of magnetization [5]. Powerful chalcogenide spinel platforms containing the 227 (Fd-3m space group) have garnered attention in the realm of hypothetical chalcogenides owing to their notable attributes, including stability, substantial basic electrical conductance, and phasing strength [6-8]. Calcogneide spinels generally possess a chemical structure of AB_2X_4 due to an octal arrangement in which (B^+) ions coordinate via chalcogenide X- ions. For instance, $(O, S, Se)^{2-}$ forms an externally shared AB_2X_4 octahedral in which A^+ ions are typically located on tetrahedral organised locations. This configuration

* Corresponding author: saba.maq.55@gmail.com
https://doi.org/10.15251/CL.2024.216.449

facilitates the establishment of a three-dimensional (3D) structure that includes dispersion channels. The spinels in question exhibited intriguing electric and magnetic properties [9]. Spinels are, for the most part, exceptionally thermodynamically as well as physically stable substances at ambient temperature. Chalcogenide, which mimics mixed-metal spinels, is particularly noteworthy for its potential as an initiator in multiple applications. Spinels possess remarkable physical and chemical features and frequently engage in redox reactions, rendering them potentially valuable in addressing energy-related issues [10].

Exploration ought to be conducted into unique ferromagnetic substances that function at ambient temperature and exhibit spin polarity at the Fermi point in order to develop functional spintronics products. According to reports, AB_2X_4 ferrous compounds are the most efficient component for spin electronics. The utilisation of the spintronics, that involves the disclosure, recording, and transmission of data via spins in substances based on spins, contributes to the expansion of micro-electronic technology applications in science and engineering [11, 12]. Semiconductors organised according to ferromagnetism have the ideal compounds for use in spintronics. A multitude of semiconductor-based substances with broad bandgaps can be seeded with magnetic components to generate novel, spintronics friendly properties by inducing local ferromagnetic sequence [13, 14]. The ferromagnetic characteristics of the aforementioned spinels are more apparent in comparison to those of traditional materials, such as $MgYb_2S_4$ [15]. Favoured were ferromagnetic spinels alongside semiconductor electronical properties [16, 17] due to their application in the spintronics, ferroelectrics, and storage devices. Due to their gigantic magneto-resistance (GMR) characteristic, rare earth-based ferro-spinels are of particular curiosity to researchers [18, 19]. GMR compounds find extensive application in various sectors, including but not limited to hard discs, detectors, spin valves, or electronic equipment. In order to enhance the performance of electric parts and devices, it is imperative to conduct a comprehensive investigation into the arrangement and spin polarisation of the electric charges within these substances.

$CdEr_2S_4$ and $CdEr_2Se_4$ are two types of thio-spinel structures that have been observed, based on prior research [20, 21]. While this provides an excellent foundation for investigating the basic principles of Cd^{2+} an exclamation point, the practical voltages are inadequate to generate Cd cells operating at exceptionally high energy. There has been a lack of current scientific inquiry into the chalcogenide spinels $CdSm_2(S/Se)_4$, which are extremely rare-earth Cd^{2+}-based, in accordance to a few claims. The available research on the structural characteristics of the two spinels is extremely limited, which complicates an organised examination [22]. In the interim, it is imperative to further comprehend the spin-polarized electronic properties of these chalcogenides in order to precisely ascertain their potential uses in the field of spintronics. Therefore, a comprehensive theoretical analysis is undertaken to examine the mechanical, electronic, as well as magnetic properties of chalcogenide spinels $CdSm_2(S/Se)_4$. The aforementioned reports exhibited encouraging characteristics of Cd-based spinels. The current research nonetheless fails to conduct a comprehensive investigation into the half-metallic (HM) ferromagnetism of the suggested chalcogenides. In this study, we conducted an exhaustive investigation into the electronic composition, Curie temperature, spin polarisation, HM ferromagnetism, of $CdSm_2(S/Se)_4$ chalcogenides. FM is being identified as an outcome of an exchange process, and the Sm material exhibits entire spin polarisation without any discernible cluster effect.

2. Calculations methodology

Hence, a detailed theoretical investigation of the optoelectronic, thermal, mechanical, and magnetic characteristics of $CdSm_2(S/Se)_4$ chalcogenides, is conducted. The DFT-based WIEN2k software package has been employed to calculate the structural, electrical, elastic, and magnetic properties of $CdSm_2(S/Se)_4$ chalcogenides since it is critical for examining their potential for spintronics application [23]. The studied chalcogenides accurate electronic structures and calculated band gaps are computed using the WIEN2k algorithm [24]. The structure of these spinels will strongly support the fabrication and implementation of spintronics devices. For the evaluation of ferromagnetic PBEsol-GGA approach were utilised. The utilisation of the GGA

estimate method was recently implemented to optimise the structural characteristics. As the GGA assumption undervalues the electrical band gap [25], the modified Becke and Johnson potential variant mBJ potential is being implemented to obtain precis eelectronically band shapes. The mBJ is utilised for calculating the electromagnetic band structures. This version provides greater accuracy compared to the GGA+U potentials. This potential becomes more precise and adaptable; it clarifies the exchange relationship among d and f electrons [26]. In this type of evaluation, spherical harmonies present in muffin-tin orbs had been commonly employed in conjunction with plane waves that were emanating from interstitial areas. RMT × Kmax = 8 and Gmax = 24 Ry^{-1} were selected with the power convergence specifications of 0.00001 Ry in order to achieve the maximum energy convergence. In contrast, DOS (density of states) and band structures were modified to include k-mesh (12×12×12).

3. Results and discussion

The optimized parameters such as lattice constant (a_0) and the bulk modulus (B_0) in ferromagnetic states were successfully ascertained through the application of Murnaghan's formulation of state, as detailed in Table 1. In the ferromagnetic phase, the optimized lattice constant of $CdSm_2(S/Se)_4$ chalcogenides follow similar trend to the earlier investigated lattice parameter of $CdEr_2X_4$ (X= S, Se) [27]. The bulk modulus decreases from $CdSm_2S_4$ to $CdSm_2Se_4$, whereas the value of the lattice constant rises due to the fact that the inter-atomic spacing expands in proportion to the magnitude of an anion. As shown in Figure 1, the cubic state of chalcogenides $CdSm_2(S/Se)_4$ has a repetitive crystal form containing a space group called 227 Fd-3m.

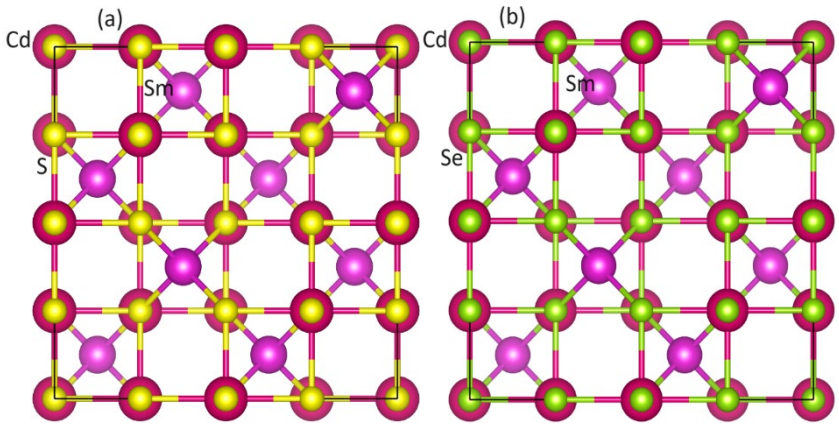

Fig. 1. Chalcogenides crystal structure of (a) $CdSm_2S_4$ and (b) $CdSm_2Se_4$.

The optimal energy versus volume of the substance in its ferro-magnetic, anti-ferromagnetic, and not magnetic orbits has been determined using Murnaghan's equation of state (refer to Fig. 2). Utilising the equation $\Delta E = E_{AFM}-E_{FM}$, the energy differences between the previously mentioned chalcogenides in their ferro-magnetic (FM) and anti-ferromagnetic (AFM) modes were computed. The arrangement of the magnetization moments in $CdSm_2(S/Se)_4$ is elucidated for both ferro-magnetic (FM) and anti-ferromagnetic (AFM) constructions, with the spins remaining identically parallel and opposite between Sm elements, respectively. An observation can be made that the ferromagnetic state emits a greater amount of energy in comparison to the anti-ferromagnetic (AFM) (see Figure 2). This observation implies the fact that the ferro-magnetic (FM) phases exhibits greater thermal stability in comparison with the anti-ferromagnetic domains.

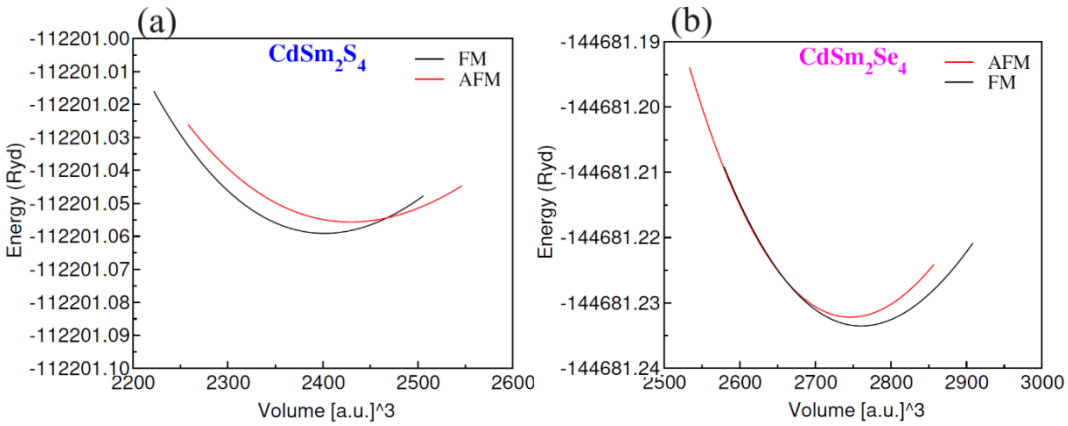

Fig. 2. Chalcogenides energy versus volume plot in ferromagnetic (FM) and anti-ferromagnetic (AFM) phases for (a) $CdSm_2S_4$ and (b) $CdSm_2Se_4$.

The temperature known as Curie Tc was determined through the utilisation of mean-field estimations $k_B T_C = \frac{2}{3}\Delta E$ and distorting the Heisenberg simulation [28]. In this calculation, ΔE represents the quantity of energy disparity between the FM or AFM arrangements, k_B and T_c denote the Boltzmann coefficient as well Curie temperature, respectively. FM rotations are considered to be more auspicious in comparison to AFM orbital motion. Table 1 presents predicted Tc values, which align with the recently documented span from 600 towards 1000 K [29]. The elevated Tc values of the investigated chalcogenides is due to the substantial energy difference (ΔE) that exists between both the FM and AFM phases. The lattice distribution spectrum of the $CdSm_2(S/Se)_4$ crystal arrangement was recently ascertained in order to assess its structural stability. The thermal resistance of the investigated materials has been determined through the measurement of the creation energy (ΔH_f); the calculated values are provided in Table 1. The observed lower energy values of the formation enthalpy for the particular spinels under investigation indicate that they are exceptionally stable. To ascertain the structure, the subsequent equation [30] was utilized.

$$\Delta H_f = E_{\text{Total}}\left(\text{Cd}_l Sm_m\, S/Se_n\right) - \text{lE}_{\text{Cd}} - \text{mE}_{\text{Sm}} - \text{nE}_{S/Se} \quad (1)$$

E_{Total} denotes the aggregate energy of $CdSm_2(S/Se)_4$, while E_{Cd}, E_{Sm}, while $E_{S/Se}$ describe the energy content for each of the atoms. The unit volume of each cell of $CdSm_2(S/Se)_4$ is denoted by the letters l, m, and n, which represent the appropriate number of elements of Cd, Sm, and S/Se. Furthermore, it is observed that the anticipated formation energy declines from -1.92 eV to -1.25 eV if the Se anion is substituted for the S anions. The stability of the chemicals being studied is noteworthy, as indicated by their formation energy levels that are approximated to be minus. This is additionally supported by the stated phase constancy of the $CdSm_2(S/Se)_4$ structure, which has been demonstrated to be steady with respect to various chemical compositions including Cd, Sm, and S.

Table 1. The calculated lattice parameters, bulk modulus values, the ground-state energy differences, Curie Temperature (T_c) and formation energy (ΔH_f) of $CdSm_2(S/Se)_4$ chalcogenides.

Chalcogenides	a_o(Å)	B_o(GPa)	$\Delta E_1 = E_{AFM}-E_{FM}$	T_c	ΔH_f
$CdSm_2S_4$	11.29	11.78	44.65	680	-1.92
$CdSm_2Se_4$	61.72	51.43	28.46	630	-1.25

The physical features of a substance are delineated by its elastic attributes. The physical parameters of a substance govern its elastic properties due to the correlation among the durability of its atomic links and its elastic coefficient. The material's physical properties ascertained through the PBEsol method may, as anticipated, furnish further illuminating data regarding the dimensional longevity of $CdSm_2(S/Se)_4$ [31]. The elasticity modulus were computed utilising the data from tensor matrices observations in order to comprehensively assess the structural strength of the substances under investigation. The cubic structure's elasticity characteristics are delineated through the utilisation of three distinct elastic parameters: C_{11}, C_{12}, and C_{44}. By switching Se for S in the analysed spinels, a highly stable $CdSm_2S_4$ is produced; this results in a reduction in the elastic capacities of(C_{11}, C_{12}, and C_{44}). The Born requirements, which are as follows: criteria (C_{11} - $C_{12} > 0$, $C_{12} < B_0 < C_{11}$, $C_{44} > 0$, and $C_{11} + 2C_{12} > 0$) are applicable to cube-shaped systems utilised in the investigation of spinels' stabilisation. Positive outcomes were observed concerning the spinels under study [32]. In addition, the energy consumption is optimised using Murnaghan's equation-of-state (EOS) and the calculation $B_0 = (C_{11}+2C_{12})/3$ the resultant bulk coefficients numbers are consistent.

The computed physical or mechanical features demonstrate how the morphological uniformity of the substances being studied has been confirmed, as well as their fundamental and elastic attributes exhibit an obvious connection. To be applicable in energy products, a substance requires flexible properties. The investigation involves the assessment of the elasticity and stiffness of the power source spinels under consideration via Poisson's ratio (υ). In general, an acceptable threshold of 0.26 is taken into account. Typically, materials exhibit brittleness and ductility when their upper limit is both greater than and less than this figure. The elastic nature of $CdSm_2Se_4$ and $CdSm_2S_4$ is supported by the associated Poisson's ratio ratios of 0.40 and 0.39. Similarly, the evaluation of a substance's fragility and elasticity typically involves the application to the Pugh ratio ((B_0/G), which has a crucial value of 1.75 [33]. Once more, the estimated values for ductility for $CdSm_2Se_4$ and $CdSm_2S_4$ are 4.85 and 4.39, accordingly. Furthermore, comparative study reveals that $CdSm_2S_4$ exhibits greater ductility in comparison to $CdSm_2Se_4$. In addition, the anisotropic (A) attribute of the investigated spinels is computed using the elasticity coefficients $A = 2C_{44}/(C_{11}-C_{12})$, the material is isotropic if A = 1, whereas it is anisotropic otherwise. The rise in the A ratio from S to Se is illustrated in Table two. Researchers may utilise the results of elastic variable measurements in the cubic form as a hypothetical instrument for manufacturing and designing.

Table 2. Calculated elastic constant (C_{11}, C_{12}, C_{44}) for chalcogenides $CdSm_2(S/Se)_4$ and their calculated bulk modulus (B), Shear modulus (G), Young Modulus (Y), Poisson's ratio (υ),Pugh ratio ((B_0/G) and anisotropic (A).

	C_{11}	C_{12}	C_{44}	B_0	G	Y	B_0/G	υ	A
$CdSm_2S_4$	109.80	35.33	5.68	60.15	13.34	37.54	4.47	0.39	0.15
$CdSm_2Se_4$	92.62	27.88	3.45	49.46	10.19	28.61	4.85	0.40	0.11

The determination of a magnetic material's practical utility can be achieved by analysing its spin-polarized electric properties. In order to discern and comprehend the electric properties of chalcogenides $CdSm_2(S/Se)_4$ mBJ potentials were utilized to compute the electric barrel configurations. In order to provide a precise representation of the electric properties, the patterns of bands are computed utilizing the mBJ method, as visually represented in Figure 3.

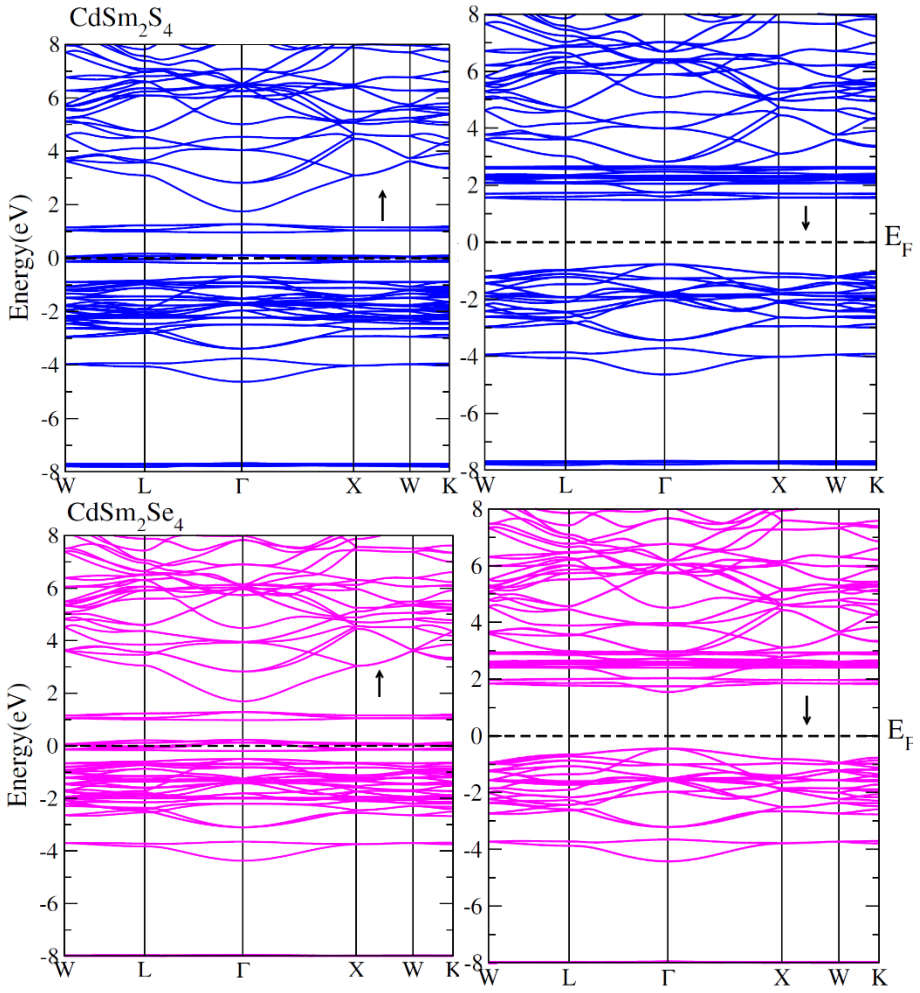

Fig. 3. Spin-polarized band structures for $CdSm_2(S/Se)_4$ in minority (↓) and majority (↑) spin channels).

The maximal frequency band and minimal conductivity band of the spin-up channels are located at the Fermi lines. An investigation is being conducted on the first-order band to spin down that is produced at the Γ-point in relation to both the peaks and troughs of the conducting bands. Discovered at the core of the electronically band structure comprises the Fermi levels. By means of the switching mechanism, a shielding band gap is produced. In broad terms, the spin-down characteristic signifies the semiconductor's nature, while the spin-up characteristic, which represents a metal's nature, interacts to produce a half-metallic FM materials characteristic [34]. An analogous pattern of FM semiconductors in $CdSm_2S/Se_4$ spinels composed of rare-earth elements was previously documented [35]. The determined spin-up direct band gaps values of both substances, denoted in Table 1 as mBJ potential, are critical for their prospective implementation in applications involving optical electronics.

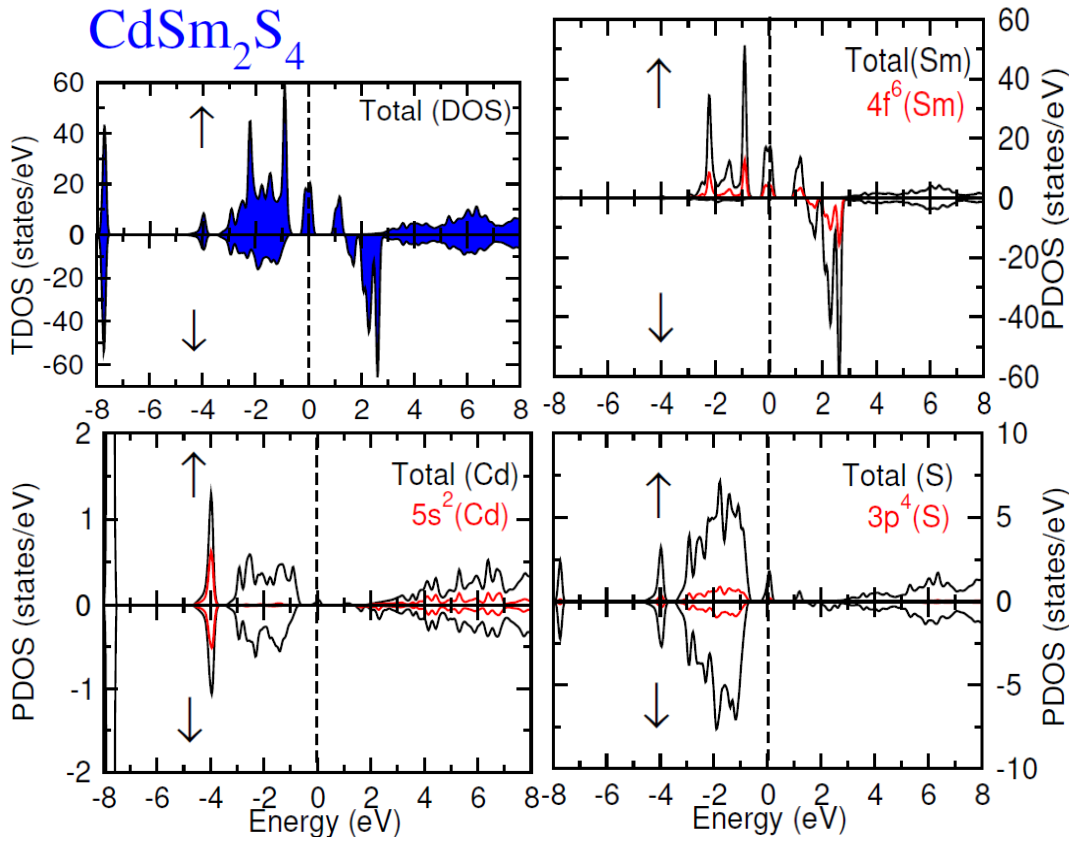

Fig. 4. TDOS and PDOS calculated for $CdSm_2S_4$ spinels (spin down (↓) and spin up (↑) orientation).

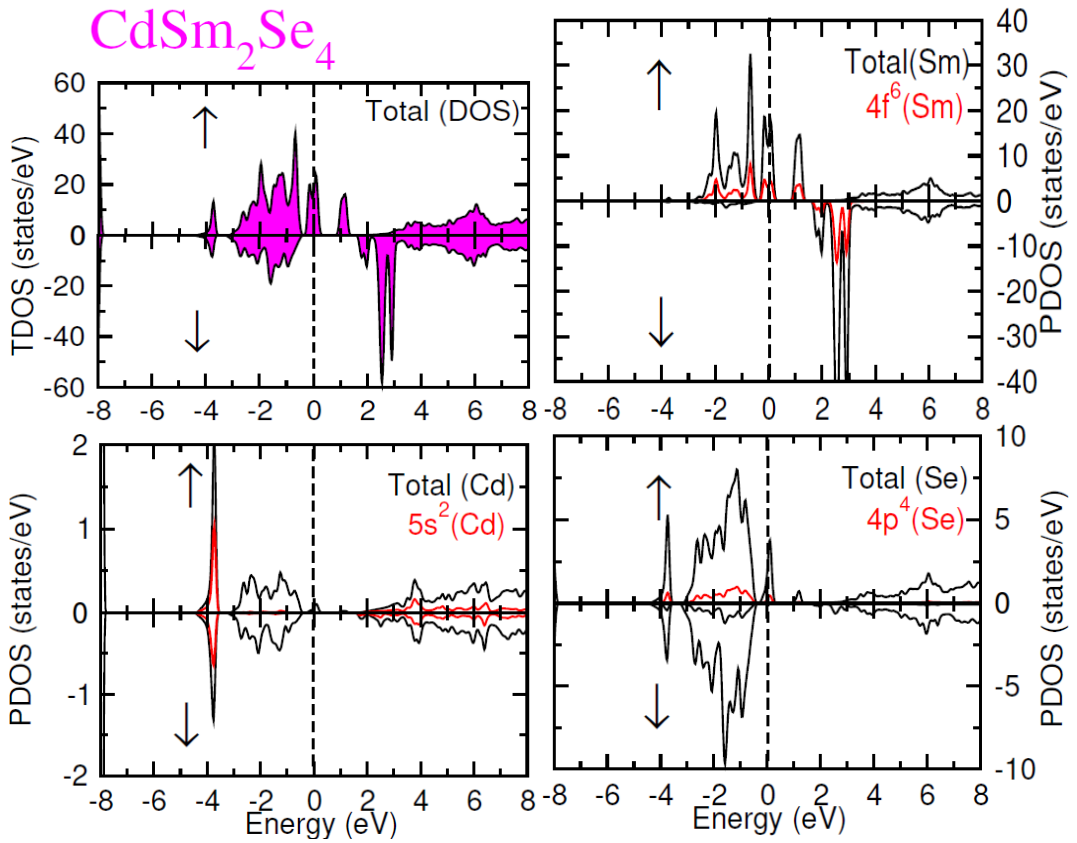

Fig. 5. TDOS and PDOS calculated for $CdSm_2Se_4$ spinels (spin down (↓) and spin up (↑) orientation).

An analysis of the DOS-plot is conducted by considering both full and fractional DOS, as illustrated in Figures 4 and 5. Particular Cd-$5s^2$ and Sm-$4f^6$ orbits hybridise with S/Se-$4p^4$in the spin-up channels at energies of -4.5 to 6.1 eV and -2.8 to 3.0 eV, correspondingly. Furthermore, spin-down channels inversion is observed in the conduction spectrum region between 0.2 and 1.3 eV for the Cd-$5s^2$ and Sm-$4f^6$ orbits, along with to the S/Se-$2/3p^4$ cycles. On the other hand, spin-up channels inversion transpires between 2.0 and 2.4 eV. Statistical investigations of the band's characteristics, such as the borders of both valence as well as conduction bands, are feasible due to their significance nature in a multitude of cubic elements [36, 37]. FM phases appear steadier than AFM along with paramagnetic spin values due to the greater energy released by ferro-magnetic organised spin trajectories.

Furthermore, in order to preserve the characteristics of FM materials, the energy transfer throughout the network is predominantly governed by the diminishing energy in ferro-magnetic and non-ferromagnetic solids. Intriguing are uncommon earth magnetic spinels on account of their substantial involvement in the bulk moment of magnetism. In order to investigate the magnetised characteristics of $CdSm_2(S/Se)_4$, the mBJ approach was employed to calculate the local magnetization moments (LMMs) for every single component (M_{Sm}, M_{Cd}, M_S, and M_{Se}) and the overall magnetization moment (TMM) M_{tot}. This ferromagnetic diode characteristics of the electrical band formations are a result of the silicon-based nature of the spin-up conduits. The vector of motion of particles between both the conduction and VB is consequently proportional to the constant moment of magnetism. Moreover, within a magnetic substance characterised by entire spin polarisation and a constant magnetised moment, the electron's spin mobility is ensured to be entirely realised by the location of the spin-up along with spin-down components. The investigated compounds therefore exhibit TMMs of approximately $10\mu_B$ (where, μ_B = Bohr magneton) and its FM characteristics precisely correspond to this numerical value. The quantities of the overall and localised moments of magnetism are detailed in Table 2. In the occurrence of the uncommon earth element Sm, the total magnetism tends to be substantially increased. Cd and S/Se elements, conversely, contribute substantially to the overall magnetic force. Thus, the establishment of consistent ferromagnetism was achieved. The amalgamation occurs due to the electromagnetic motility exhibited by various rare-earth atomic particles, which causes a modification in the bonding orbit of Sm. Solid interactions between the p-orbits of host metals and the d-orbits about rare-earth forms generate moments of magnetization in Cd and S/Se atoms. Sm demonstrates atomically behaviour resembling that of magnets due to the substantial FM interchange separation observed within the spinels under investigation. The ferromagnetic nature of the composites is confirmed through the relationship among Cd and S/Se components.

Table 3. Magnetic moments value for chalcogenides $CdSm_2(S/Se)_4$, total and their local M_{Cd}, M_{Sm}, and $M_{S/Se}$, interstitial (M_{Int}).

	M_{Total}	$M_{Int.}$	M_{Cd}	M_{Sm}	$M_{S/Se}$
$CdSm_2S_4$	10.000	0.139	0.011	5.030	-0.0384
$CdSm_2Se_4$	10.000	0.043	0.008	5.107	-0.0913

4. Conclusion

The present investigation utilised computations using DFT to analyse the physical features of the chalcogenide spinels $CdSm_2(S/Se)_4$. To determine the physical stability of a spinels, the constant for elasticity are computed. It was determined that the Poisson as well as Pugh's ratios for $CdSm_2Se_4$ and $CdSm_2S_4$ substances had been both larger than 0.26 and 1.75, correspondingly, which provides further evidence for their elastic nature. This discrepancy between ground-state contends of ferro-magnetic and anti-ferromagnetic modes of spinels indicates that the former possessed a FM arrangement. Moreover, the ferromagnetic performance at ambient temperature was predicted by the Curie temperature (Tc) computations. Significant hybridization and

excitation connections, as determined by mBJ potential, suggest that what is causing the observable half-metallic ferromagnetic is the result of anti-symmetric electronic spin.

Funding:

Researchers Supporting Project number (RSP2024R410), King Saud University.

Acknowledgements

We extend our appreciation to the Researchers Supporting Project (RSP2024R410), King Saud University, Riyadh, Saudi Arabia.

References

[1] M. Liu, Z. Rong, R. Malik, P. Canepa, A. Jain, G. Ceder, K. A. Persson, Energy Environ. Sci. 8 (2015) 964-974; https://doi.org/10.1039/C4EE03389B

[2] Z. Rong, R. Malik, P. Canepa, G. Sai Gautam, M. Liu, A. Jain, K. Persson, G. Ceder, Chem. Mater. 27 (2015) 6016-6021; https://doi.org/10.1021/acs.chemmater.5b02342

[3] A. Wustrow, B. Key, P.J. Phillips, N. Sa, A.S. Lipton, R.F. Klie, J. T. Vaughey, K. R. Poeppelmeier, Inorg. Chem. 57 (2018) 8634-8638; https://doi.org/10.1021/acs.inorgchem.8b01417

[4] N.W. Grimes, Phys. Technol. 6 (1975) 22; https://doi.org/10.1088/0305-4624/6/1/I02

[5] O. Vozniuk, T. Tabanelli, N. Tanchoux, J. M. M. Millet, S. Albonetti, F. Di Renzo, F. Cavani, Catalysts 8 (2018) 332; https://doi.org/10.3390/catal8080332

[6] G. Harbeke, H. Pinch, Phys. Rev. Lett. 17 (1966) 1090; https://doi.org/10.1103/PhysRevLett.17.1090

[7] N.A. Noor, M. Rashid, Ghulam M. Mustafa, Asif Mahmood, Waheed Al-Masry, Shahid M. Ramay, J. Alloys Compd., 856 (2021) 157198; https://doi.org/10.1016/j.jallcom.2020.157198

[8] H. Göbel, J. Magn. Magn. Mater. 3 (1976) 143- 146; https://doi.org/10.1016/0304-8853(76)90025-1

[9] A. Gaita-Ariño, F. Luis, S. Hill, E. Coronado, Nature chemistry, 11 (2019), 301-309; https://doi.org/10.1038/s41557-019-0232-y

[10] S. Sun, H. Zeng, D.B. S. Robinson, Raoux, P.M. Rice, S.X. Wang, G. Li, J. Am. Chem. Soc. 126 (2004) 273- 279; https://doi.org/10.1021/ja0380852

[11] Q. Mahmood, S. M. Alay-e-Abbas, M. Hassan, N.A. Noor, Journal of Alloys and Compounds, 688 (2016) 899-907; https://doi.org/10.1016/j.jallcom.2016.07.302

[12] T. Seddik, R. Khenata, A. Bouhemadou, N. Guechi. A. Sayede, D. Varshney, Y.Al-Douri, A.H. Reshak, S. Bin-Omran, Physica B 428 (2013) 78-88; https://doi.org/10.1016/j.physb.2013.07.014

[13] V. Samokhvalov, M. Dietrich, F. Schneider, S. Unterricker, Hyperfine Interactions 160 (2005) 17-26; https://doi.org/10.1007/s10751-005-9146-8

[14] Y.D. Park, A.T. Hanbicki, J.E. Mattson, B.T. Jonker, Appl. Phys. Lett. 81N8 (2002) 1471; https://doi.org/10.1063/1.1498503

[15] G. C. Lau, R. S. Freitas, B. G. Ueland, P. Schiffer, R. J. Cava, Phys.Rev. B 72, (2005) 054411; https://doi.org/10.1103/PhysRevB.72.054411

[16] P. Lunkenheimer, R. Fichtl, J. Hemberger, V. Tsurkan, A. Loidl, Phys. Rev. B 72 (2005) 060103; https://doi.org/10.1103/PhysRevB.72.060103

[17] C. P. Sun, C.L. Huang, C. C. Lin, J. L. Her, C. J. Ho, J. Y. Lin, H. Berger, H. D. Yang, Appl.

Phys. Lett. 96 (2010) 122109; https://doi.org/10.1063/1.3368123

[18] Y. M. Xie, Z. R. Yang, L. Li, L. H. Yin, X. B. Hu, Y. L. Huang, H. B. Jian, W. H. Song, Y. P. Sun, S. Q. Zhou, Y. H. Zhang, J. Appl. Phys.112 (2012) 12391; https://doi.org/10.1063/1.4770486

[19] R. von Helmolt, J. Wocker, B. Holzaphel, M. Scholtz, K. Samwer, Phys. Rev lett. 71, (1993) 2331.

[20] Lau, G. C., R. S. Freitas, B. G. Ueland, P. Schiffer, R. J. Cava. Physical Review B 72, no. 5 (2005): 054411; https://doi.org/10.1103/PhysRevB.72.054411

[21] Lago, Jorge, I. Živković, B. Z. Malkin, J. Rodriguez Fernandez, Paolo Ghigna, P. Dalmas De Réotier, A. Yaouanc, T. Rojo. Physical review letters 104, no. 24 (2010): 247203; https://doi.org/10.1103/PhysRevLett.104.247203

[22] A. Jain, S. P. Ong, G. Hautier, W. Chen, W. D. Richards, S. Dacek, S. Cholia, D. Gunter, D. Skinner, G. Ceder, K. A. Persson, APL Materials, 1 (2013) 011002; https://doi.org/10.1063/1.4812323

[24] P. Blaha, K. Schwarz, G.K.H. Madsen, D. Kvasnicka, J. Luitz, WIEN2K, An Augmented Plane Wave + local Orbitals Program for Calculating Crystal Properties, Karlheinz Schwarz, Techn. Universiẗat Wien, Austria, 2001

[25] P. Perdew, A. Ruzsinszky, G. I. Csonka, O. A. Vydrov, G. E.Scuseria, L. A. Constantin, X. Zhou, K. Burke, Phys. Rev. Lett. 100 (2008) 136406; https://doi.org/10.1103/PhysRevLett.100.136406

[26] F. Tran, P. Blaha, Phys. Rev. Lett. 102 (2009) 226401; https://doi.org/10.1103/PhysRevLett.102.226401

[27] Alburaih, H. A., Journal of Alloys and Compounds 876 (2021): 159806; https://doi.org/10.1016/j.jallcom.2021.159806

[28] F. Máca, J. Kudrnovský, V. Drchal, G. Bouzerar, Appl. Phys. Lett. 92 (2008) 212503; https://doi.org/10.1063/1.2936858

[29] W. Z. Xiao, G. Xiao, Q. Y. Rong, Q. Chen, L. L. Wang, J. Magn. Magn. Mater. 438 (2017) 152-62; https://doi.org/10.1016/j.jmmm.2017.04.090

[30] B.R. Nag, Electron Transport in Compound Semiconductors; Springer Science & Business Media, 2012; Vol. 11.

[31] W. Tahir, G. M. Mustafa, N. A. Noor, S. M. Alay-e-Abbas, Q. Mahmood, A. Laref, Ceramics International, 46 (2020), 26637-26645; https://doi.org/10.1016/j.ceramint.2020.07.133

[32] Farzana Majid, M. Tauqeer Nasir, Eman Algrafy, Muhammad Sajjad, N. A. Noor, Asif Mahmood, Shahid M.Ramay, J. Mat. Res. Tech. 9 (2020) 6135-6142; https://doi.org/10.1016/j.jmrt.2020.04.016

[33] X. Ji, Y. Yu, J. Ji, J. Long, J. Chen, D. Liu, J. Alloy Compd. 623 (2015)304; https://doi.org/10.1016/j.jallcom.2014.10.151

[34] N. Abbouni, S. Amari, H. Sadouki, A. Belkadi, Y. Zaoui, K. O. Obodo, L. Beldi, B. Bouhafs, Spin, 8, (2018) 1850020; https://doi.org/10.1142/S2010324718500200

[35] N. A. Noor, M. Arslan Majeed, M. Aslam Khan, Shanawer Niaz, M. Waqas Iqbal, Taswar Abbas, A. Dahshan, Materials Science in Semiconductor Processing, 149 (2022) 106861; https://doi.org/10.1016/j.mssp.2022.106861

[36] M. Roknuzzaman, K. Ostrikov, H. Wang, A. Du, T. Tesfamichael, Sci. Reports 7(2017) 14025; https://doi.org/10.1038/s41598-017-13172-y

[37] G. Hayatullah, R. Murtaza, S. Khenata, S. Mohammad, M. N. Naeem, A. Khalid, Manzar, Phys. B 420 (2013) 15; https://doi.org/10.1016/j.physb.2013.03.011